Cerebral Cortex, October 2016;26: 3953–3963

doi: 10.1093/cercor/bhw233
Advance Access Publication Date: 13 August 2016
Original Article

ORIGINAL ARTICLE

Longitudinal Evidence for Dissociation of Anterior and Posterior MTL Resting-State Connectivity in Aging: Links to Perfusion and Memory

Alireza Salami[1,2,4], Anders Wåhlin[1,3], Neda Kaboodvand[1,4], Anders Lundquist[1,2], and Lars Nyberg[1,2,5]

[1]Umeå Center for Functional Brain Imaging, S-90187, Umeå, Sweden, [2]Department of Integrative Medical Biology, Physiology Section, Umeå University, S-901 87 Umeå, Sweden, [3]Department of Radiation Sciences, Radiation Physics, Umeå University, S-901 87 Umeå, Sweden, [4]Aging Research Center, Karolinska Institutet and Stockholm University, SE-113 30, Stockholm, Sweden, and [5]Department of Radiation Sciences, Diagnostic Radiology, Umeå University, S-901 87 Umeå, Sweden

Address correspondence to Alireza Salami, Department of Integrative Medical Biology, Center for Functional Brain Imaging, Umeå University, S-901 87 Umeå, Sweden. E-mail: alireza.salami@physiol.umu.se

Abstract

Neuroimaging studies of spontaneous signal fluctuations as measured by resting-state functional magnetic resonance imaging have revealed age-related alterations in the functional architecture of brain networks. One such network is located in the medial temporal lobe (MTL), showing structural and functional variations along the anterior–posterior axis. Past cross-sectional studies of MTL functional connectivity (FC) have yielded discrepant findings, likely reflecting the fact that specific MTL subregions are differentially affected in aging. Here, using longitudinal resting-state data from 198 participants, we investigated 5-year changes in FC of the anterior and posterior MTL. We found an opposite pattern, such that the degree of FC within the anterior MTL declined after age 60, whereas elevated FC within the posterior MTL was observed along with attenuated posterior MTL-cortical connectivity. A significant negative change–change relation was observed between episodic-memory decline and elevated FC in the posterior MTL. Additional analyses revealed age-related cerebral blood flow (CBF) increases in posterior MTL at the follow-up session, along with a positive relation of elevated FC and CBF, suggesting that elevated FC is a metabolically demanding alteration. Collectively, our findings indicate that elevated FC in posterior MTL along with increased local perfusion is a sign of brain aging that underlie episodic-memory decline.

Key words: episodic memory, functional connectivity, longitudinal, anterior and posterior MTL, perfusion

Introduction

Aging is associated with declining cognitive performance (Nilsson et al. 1997; Nyberg et al. 2003; Nilsson et al. 2004) and concomitant alterations in brain structure (Raz et al. 2005; Fjell et al. 2009; Salami et al. 2011), dopaminergic neurotransmission (Bäckman et al. 2006; Bäckman et al. 2010), cerebral blood flow (CBF) (Zarrinkoob et al. 2015), metabolism (Kalpouzos et al. 2009; Segobin et al. 2015), and task-induced functional activation across various cognitive domains (Grady 2012; Salami et al. 2012; Nyberg et al. 2014; Salami et al. 2013). In addition, neuroimaging studies of spontaneous fluctuations in blood oxygen level-dependent signal (BOLD) measured by

resting-state functional magnetic resonance imaging (fMRI) have revealed age-related alterations in the functional coupling of distal brain regions (Andrews-Hanna et al. 2007; Damoiseaux et al. 2008; Biswal et al. 2010; Allen et al. 2011; Mowinckel et al. 2012; Geerligs, Renken, et al. 2014; Salami et al. 2014; Ferreira et al. 2015). Relative to younger adults, older adults show decreased functional connectivity (FC) in several cortical resting-state networks (RSNs), including the fronto-parietal control network and the cortical default mode network (DMN; for a comprehensive review, see Ferreira and Busatto 2013).

Within the DMN, which entails interactive subsystems and hubs (Buckner et al. 2008; Andrews-Hanna et al. 2010; Campbell et al. 2013), the direction of differences in FC has not only been age-related decline but also age-related elevation (Westlye et al. 2011; Campbell et al. 2013; Ferreira and Busatto 2013; Eavani et al. 2016). In particular, the anterior and posterior cortical DMN have been found to show age-related decline (Andrews-Hanna et al. 2007; Damoiseaux et al. 2008; Salami et al. 2014). In the bilateral medial temporal lobe (MTL), both increases and decreases in aging have been reported. Age-related increases in FC were observed between MTL regions in a cross-sectional fMRI study (Salami et al. 2014). Similarly, a combined fMRI/electroencephalography study reported age-related increase in hippocampus (HC) electroencephalography beta power during rest (Balsters et al. 2013). Conversely, age-related decreases in MTL FC and efficiency have been reported in other studies (Achard and Bullmore 2007; Toussaint et al. 2014). One possible explanation for discrepant findings regarding MTL FC could be that specific MTL subregions are differentially affected in aging (Small et al. 2011). Several previous human and animal studies have revealed structural and functional variations along the anterior–posterior axis of the HC (Moser and Moser 1998; Poppenk and Moscovitch 2011; Blessing et al. 2015; Damoiseaux et al. 2016; Moscovitch et al. 2016), which have been further corroborated on a fine-grained scale using high-resolution fMRI in young (Kahn et al. 2008; Libby et al. 2012) and older (Das et al. 2015) adults. In our previous cross-sectional study, age-related decreases in cortical DMN were seen along with increases in global FC in a large portion of the posterior MTL [pMTL (Salami et al. 2014)], whereas age-related FC decline has been seen in more anterior MTL (aMTL) subregions (Toussaint et al. 2014). To the best of our knowledge, longitudinal data on age-related alterations across distinct MTL regions are lacking. Therefore, our primary aim here was to investigate whether 5-year longitudinal changes would differentially impact FC in aMTL and pMTL, as well as in cortical DMN, and in particular whether longitudinal evidence would be obtained for elevated FC in the pMTL (cf., Salami et al. 2014).

Previous studies have reported coupling of FC and regional CBF, which speaks to the physiological basis of FC (Liang et al. 2013; Jann et al. 2015; Passow et al. 2015). We previously hypothesized that increased pMTL FC could be due to progressively less inhibitory cortical input (Salami et al. 2014; see also Das et al. 2013). Relatedly, a recent animal study showed that cortical inhibitory projection promotes the excitation of hippocampal neurons (Basu et al. 2016). It has also been proposed that HC subregions are vulnerable to age-related loss of inhibitory input, which cascades into HC hyperactivation (Leal and Yassa 2013). Relatedly, MTL hyperperfusion has been reported for non-demented elderly individuals with increased genetic risk for AD (Fleisher et al. 2009), patients with MCI (Lacalle-Aurioles et al. 2014), and AD patients (Alsop et al. 2008). A second aim of this study was to investigate the link between FC and CBF in distinct MTL regions. We hypothesized that elevated MTL FC would be accompanied by local MTL hyperperfusion as well as disruption in cortico-MTL FC (the latter may be defined as different DMN subsystems, but will here be referred to in terms of internetwork connectivity).

Altered RS-FC in aging has been related to age-related memory changes (Fjell et al. 2015). Our previous cross-sectional findings indicted that elevated MTL connectivity is detrimental for episodic memory in older adults (Salami et al. 2014), but cross-sectional estimates may be biased and only a longitudinal design can directly estimate within-person change (Lindenberger et al. 2011). A third aim here was therefore to longitudinally examine the link between individual differences in 5-year change in MTL FC and 15-year change in hippocampus-based episodic long-term memory.

Methods

Subjects and Experimental Procedures

All participants in the present study were part of the *Betula* prospective cohort study on memory, health, and aging (Nilsson et al. 1997; Nilsson et al. 2004). Betula is a longitudinal study containing cognitive and medical data for nearly 4500 individuals. Within the Betula 6 waves of cognitive assessment have been conducted. The waves were completed at different time (T) points: 1988–1990 (T1), 1993–1995 (T2), 1998–2000 (T3), 2003–2005 (T4), 2008–2010 (T5), and 2013–2014 (T6). The interval between T's was approximately 5 years. At the various time points, several different samples have been included, starting with Sample 1 at T1, and Samples 2 and 3 at T2. In connection with T5, 292 participants from Samples 1 and 3 were scanned with structural and functional MRI. An additional 83 participants from a new sample recruited at T5 (Sample 5) were also included in the imaging study, adding up to 375 persons in total. From the initial sample, 37 were excluded due to technical error and/or severe motion (Frame-wise displacement >0.5) that corrupted fMRI data. All remaining participants (n = 339; 25–80 years; mean ± SD: 61.5 ± 13.3; 176 females) were native Swedish speakers, had normal or corrected-to-normal vision, and had no history of severe neurological illness or events that might cause dementia.

FMRI time series data from the participants were acquired at rest over a 6-min period. Participants were instructed to keep their eyes open during the scan and look at a presented fixation cross (for more detail, see Salami et al. 2014). The resting-state experimental design was identical at both baseline and follow-up (i.e., 6-min scanning acquired on exactly the same machine using the same head coil). Of the subjects who participated in the first imaging session, 231 completed the 2013–2014 follow-up study at T6, but only 198 subjects (30–85 years of age; mean ± SD: 64.2 ± 13.02; 93 females) were included in this study. Reasons for exclusion included depression, Parkinson's disease, and dementia.

Imaging Methods

Structural and functional imaging was performed on a 3-T General Electric scanner equipped with a 32-channel head coil. Resting-state fMRI was acquired with a gradient echo planar imaging sequence [37 transaxial slices, thickness; 3.4 mm, gap; 0.5 mm, repetition time (TR); 2000 ms, echo time (TE); 30 ms, flip angle; 80°, field of view; 25 × 25 cm, 170 volumes]. Ten dummy scans were collected and discarded before experimental image acquisition. High-resolution T1-weighted structural images were collected with a 3D fast spoiled gradient echo sequence (180

slices; thickness, 1 mm; TR, 8.2 ms; TE, 3.2 ms; flip angle, 12°; field of view, 25 × 25 cm). At the follow-up, we additionally assessed CBF data using a background suppressed, 3D pseudo-continuous arterial spin labeling (pCASL) sequence with the following settings: stack of spiral fast spin-echo read-out, 512 sampling points on 8 spirals, FOV, 240 × 240 mm^2; slice thickness 4 mm; arterial labeling at the cerebellar base; 1500 ms labeling duration, 1525 ms postlabeling delay, 30 control/label pairs. CBF maps where computed showing tissue CBF in ml/min/100 g.

MRI Data Analyses

We closely followed the longitudinal preprocessing pipeline that was carried out in our previous work (Nyberg et al. 2010). Resting-state fMRI (rs-fMRI) data of both baseline and follow-up were preprocessed using Statistical Parametric Mapping software (SPM12; Welcome Department of Cognitive Neurology, University College London, London, United Kingdom). All images were first corrected for slice timing and then rigidly aligned to the first image volume to correct for a subject's movement. A within-subject rigid registration was carried out to align structural and functional images together. Coregistered T1-images were then segmented into gray matter (GM) and white matter (WM). Then, subject-specific templates were created using diffeomorphic anatomical registration using exponentiated lie algebra DARTEL (Ashburner 2007). This was carried out by importing GM/WM images into the DARTEL space following by a 6-steps iterative procedure (without smoothing) which produce a representative template (from baseline and follow-up) for each subject. Next, a group-specific template (using DARTEL) was created from all subject-specific templates (198 subjects). Finally, coregistered rs-fMRI data were non-linearly normalized, to the group-specific template (using flow fields from 2-steps DARTEL), affine-aligned into a Montreal Neurological Institute (MNI) template, and finally smoothed using an 8-mm full width at half maximum Gaussian filter.

Preprocessed rs-fMRI data were analyzed using temporal concatenation independent component analysis (ICA) as implemented in the GIFT toolbox (Calhoun et al. 2001a, 2001b; Allen et al. 2011). ICA is a multivariate approach that extracts patterns of the brain (i.e., components) that are spatially independent but temporally coherent. As such, ICA provides a natural measure of FC for brain components. We used ICA, rather than seed-based approaches, to identify MTL networks as this data-driven method eliminates the arbitrary choice of MTL seed regions. Indeed, previous studies showed that ICA can successfully identify resting-state MTL subregions along the longitudinal axis (Blessing et al. 2015). Moreover, compared with seed-based approaches which usually reflects simple pairwise correlation, ICA simultaneously takes into account the relation between all voxel, and may provide increased sensitivity to detect subtle FC differences in aging (Koch et al. 2010). The full details of ICA analyses were given in our previous work on the baseline sample (Salami et al. 2014). In short, a time series of each voxel was initially intensity-normalized to improve test–retest reliability of subsequent ICA output (Allen et al. 2011), and then normalized data for all participants were concatenated across time. Using a whole brain mask, we adjusted the default mask, generated by ICA, in order to cover the entire MTL areas in subsequent ICA analyses. Using minimum description length algorithm, 47 independent components (ICs) were estimated. Two-step data reduction was carried out using principal component analysis (PCA1: 100 components; PCA2: 47 components). Next, the Infomax ICA algorithm (Bell and Sejnowski 1995) was conducted to optimally extract 47 ICs. The latter procedure was repeated 20 times using the ICASSO toolbox (Himberg et al. 2004), and the resulting components were clustered to estimate the reliability of the ICs. All ICs exhibited a reliability index (Iq; ranges from 0 to 1) greater than 0.90 (except one with Iq = 0.78, which was not among components of interest). Finally, a back-reconstruction using GICA3 method, which is an improved version of dual regression, was conducted (Erhardt et al. 2011). As such, time courses (TCs) and spatial maps (SMs), both in the unit of percent signal changes, were computed for each subject. There are desirable properties in GICA3 not available in the other method, including that the aggregate SM is the sum of the subject-specific SMs, analogous to a random effects model where the subject-specific effects are zero-mean distributed deviations from the group mean effect. As such, it was shown that noise-free ICA using GICA3 provides more robust results with a more intuitive interpretation (Erhardt et al. 2011). After visually inspecting the group average maps, 32 RSNs, including MTL and DMN, were identified. These RSNs showed peak activation in the GM, and exhibited low spatial overlap with the topology of potential artifacts (e.g., vascular, ventricle, motion, and susceptibility artifacts).

Finally, to identify common regions functionally connected to each other during both time points, a voxel-wise one-sample *t*-test was conducted on averaged SM of each MTL component. Thresholds were based on the distribution of voxel-wise *t* statistics to identify voxels most representative of each component (across subjects) using a gamma-mixture model fit controlling for a false-discovery rate (FDR) of 1% (Allen et al. 2011). For the MTL components, we computed 4 ICA-driven measures that reflect distinct but complementary facets of RSNs (1) Component SMs reflected the level of coactivation (connectivity) within a network in a voxel-wise manner (voxel-wise connectivity). An SM was created after the back-reconstruction step of the group ICA, which creates subject-specific maps from a corresponding group-level IC. The value of each voxel in a SM represents the degree to which the voxel is correlated with a given networks's mean TC. (2) Global indices of FC reflected a subject-specific connectivity within the entire network. As suggested by Glahn and colleagues (Glahn et al. 2010), individual 3D subject-specific SMs for each network were concatenated into a single 4D map, and the first principal eigenvector representing the subject's connectivity was calculated within a study-specific mask of the corresponding network. The mask was generated with a Gaussian/gamma-mixture model fit to the intensity histogram of group ICA for each network, controlling for an FDR of 1%. (3) The subject-specific amplitude of a TC indicated the level of activation within a network. As suggested in a paper by Allen and colleagues (Allen et al. 2012), the amplitude was computed as a joint metric (which combines scaling information from TCs and SMs) using the TC SD, a well-characterized indicator of the spread or dispersion across the entire network, and the SM maximum value, which exhibited the amplitude of the top 20 voxels (intensity was averaged to reduce the influence of noise) most strongly associated with the corresponding TC. The TCs were detrended and despiked. In addition, motion parameters were regressed out from each component's TC (see, below for more detail). (4) The internetwork functional connectivity (IFC) reflected connectivity between networks (Jafri et al. 2008). The IFC was estimated as Pearson's correlation coefficients between pairs of TCs that were detrended, despiked, and filtered using a fifth-order Butterworth low-pass

filter ($f < 0.15$). Correlations were transformed to z-scores using Fisher's transformation (Allen et al. 2011).

CBF maps from the follow-up scans were normalized using the same transformations as the follow-up rs-fMRI scan. In addition to voxel level maps, average CBF was calculated within the aMTL and pMTL regions as well as for the posterior DMN. These regions of interest where defined from binarizing group ICA maps of the corresponding networks. Note that in all analyses, statistical control with respect to brain average CBF was applied.

MTL/DMN, Noise, and Head Motion

Previous studies have shown that non-neural activity, such as motion, have systematic effects on FC (Power et al. 2012; Van Dijk et al. 2012; Buckner et al. 2013). We have carefully investigated the effect of motion (in this sample) on resting-state ICA-driven measures using the scrubbing (Power et al. 2012) and the Friston model (Yan et al. 2013) both pre- and post-ICA [see supplementary Fig. 2 and 5 in Salami et al. 2014], and found very minor differences. In the current study, additional preprocessing was carried out to remove remaining noise sources from each components TC. These include scanner induced low-frequency trends, motion variance which may not be fully captured in a single component, and other non-specific spikes (Allen et al. 2011, 2014; Di and Biswal 2014; Geerligs, Saliasi et al. 2014; Mayer et al. 2015). To do so, the linear, quadratic, and cubic trends were detrended from TCs. Then, motion parameters were regressed out. In addition, an outlier removal approach, $3D_{Despike}$ (http://afni.nimh.nih.gov/afni), was carried out to identify outliers based on the median absolute deviation. These outliers were then replaced with the best estimate using third-order spline fit. This method, which is similar to scrubbing (Power et al. 2012), has been shown to efficiently reduce the effect of motion from ICA TCs (Allen et al. 2014; Geerligs, Saliasi et al. 2014). Finally, a low-pass filter with a high-frequency cutoff of 0.15 HZ was applied. To further examine the effect of motion cleaning before ICA, motion correction based on the Friston 24-parameter model (Yan et al. 2013) was conducted before the ICA analysis.

Longitudinal Alterations in FC and Amplitude of Distinct MTL Components

To investigate longitudinal alterations in FC of the pMTL and aMTL, a 2 (aMTL vs. pMTL global FC) by 2 (baseline vs. follow-up) ANOVA was carried out following by paired *t*-test. The latter analysis was also carried out for amplitude to investigate longitudinal changes in pMTL. To adjust for multiple comparisons, Bonferroni correction for 2 (FC and amplitude) × 2 (anterior and posterior MTL) comparisons was used.

Longitudinal Changes in Episodic Memory Over 15 Years

Episodic memory was assessed with a composite of 5 episodic memory scores, measured at 5-year intervals over a period of 20 year of the Betula study. The episodic memory composite score has a priori range between 0 and 76, with a higher score indicating better cognitive function (Josefsson et al. 2012). This composite score has been used in several previous works of our groups (Salami et al. 2011; Josefsson et al. 2012; Salami et al. 2012; Pudas et al. 2014; Salami et al. 2014; Boraxbekk et al. 2015). Analyses of the internal consistency of the composite revealed a good level (Cronbach's alpha = 0.83), and the test–retest reliability was estimated to be 0.79 (Pearson correlation; Mousavi et al. 2014). Testing procedures remained constant across measurement occasions and full details have been given previously (Nilsson et al. 1997). In brief, the composite measure was based on (1) immediate free recall of 16 imperative verb–noun sentences that were enacted by the participant (e.g., "lift the book") (2) delayed cued recall of nouns from the previously enacted sentences (3) immediate free recall of 16 verbally and visually presented sentences of the same verb–noun format as in the enactment condition (4) delayed cued recall of nouns from the previously presented sentences; and (5) immediate free recall of 12 verbally presented concrete and abstract nouns (e.g., "watch; peace").

Slope Estimate

The individual slopes of cognitive change were estimated as the slope in a simple linear regression of cognitive score versus time. To avoid test–retest effects, T3 was chosen as a starting point for slope estimation for episodic memory, since Sample 3 had its first measurement at T2. This means that the individual slopes were estimated using up to 4 observations.

To investigate the change–change relation between MTL connectivity and episodic memory, a multiple regression were carried out between changes in voxel-wise FC of each MTL component and changes in episodic memory (controlled by sex, FD movement parameter, baseline episodic memory, and baseline FC).

Link Between CBF and FC in MTL

Several analyses were carried out to explore whether FC and amplitude in MTL components are related to local CBF. In the first set of analyses, we investigated voxel-wise correlation for both changes and follow-up FC of each MTL component and its local CBF using biological parametric mapping (Casanova et al. 2007). Similarly, we also explored relationships between global FC and amplitude of each MTL component with the corresponding average CBF, using multiple regression approach (controlling for brain average CBF). Finally, we investigated age-related alterations in CBF maps of the MTL components identified with ICA (controlling for GM volume).

Link Between GM Volume and FC in MTL

ICA components were used to extract averaged GM volume within each MTL component. Change–change FC–GM association were assessed through Pearson correlation coefficients. Moreover, the association between CBF and FC in the PMTL was reassessed using partial correlation controlling for GM volume changes of the pMTL. Finally, longitudinal changes in aMTL and pMTL FC were estimated using mixed model approach which allows us to adjust for time-varying GM volume.

For longitudinal alteration in FC and amplitude of distinct MTL components, Bonferroni correction for 2 (FC and amplitude) × 2 (aMTL and pMTL) comparisons was used (i.e., $P = 0.01$). For association between CBF and pMTL regions, Bonferroni correction for 2 comparisons (FC and amplitude) was used (i.e., $P = 0.025$). For all corresponding voxel-wise analyses within pMTL, we use voxel-wise $P < 0.05$ FDR (corrects for multiple tests performed over all component-specific voxels), with an extent threshold of $K > 10$ unless otherwise specified.

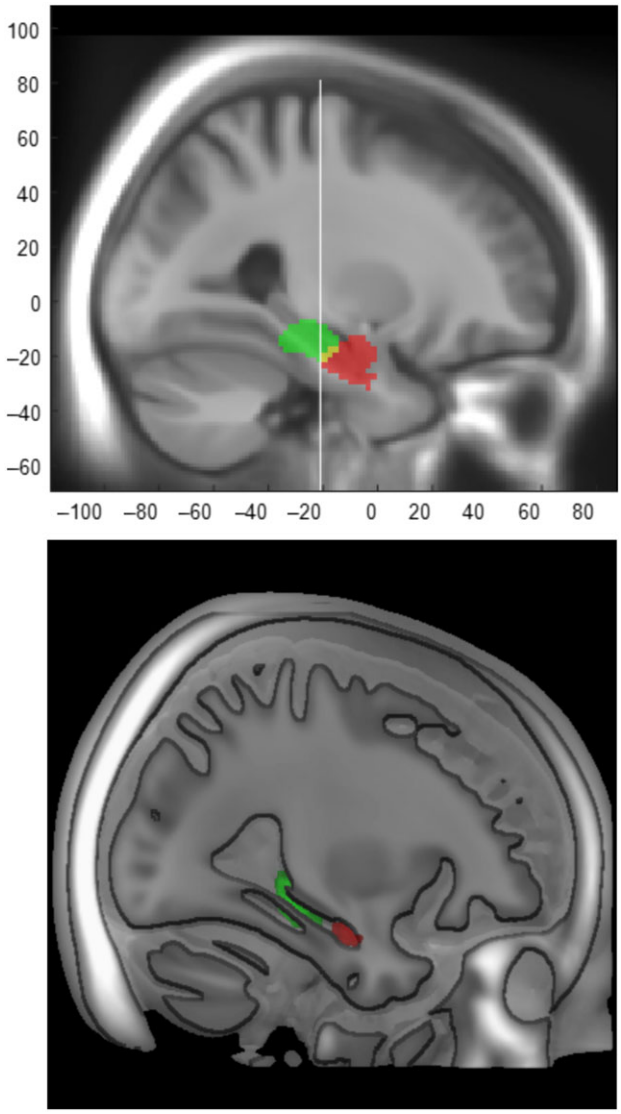

Figure 1. Two resting-state ICA components along the longitudinal hippocampal axis (2 different illustration methods). aMTL (red; left peak cluster *XYZ*: −28 −12 −20; right peak cluster *XYZ*: 28 −10 −22) and pMTL (green; left peak cluster *XYZ*: −18 −32 −14, left peak sub-cluster *XYZ*: −18 −26 −12; right peak cluster *XYZ*: 16 −30 −12, right peak sub-cluster *XYZ*: 18 −24 −10) RSNs (at the group level) are overlaid on the sample-specific template created using DARTEL. The white line represents Uncal apex landmark (Y = −21) which has been shown to be a reliable landmark for long-axis segmentation of the HC (Poppenk et al. 2013).

Results

Mapping MTL RSNs Using ICA

Our primary results stem from ICA decomposition of resting-state fMRI at a dimension of 47. This analysis resulted in highly discrete MTL components along the longitudinal hippocampal axis (aMTL vs. pMTL; Fig. 1). Critically, consistent with uncal apex landmark for long-axis segmentation of HC (Poppenk et al. 2013), aMTL included foci anterior to Y = −21 mm in MNI space (aMTL; left peak cluster *XYZ*: −28 −12 −20; right peak cluster *XYZ*: 28 −10 −22), whereas pMTL included regions posterior to Y = −21 (left peak cluster *XYZ*: −18 −32 −14, left peak sub-cluster *XYZ*: −18 −26 −12; right peak cluster *XYZ*:16 −30 −12, right peak sub-cluster *XYZ*:18 −24 −10). Moreover, 3 cortical DMN components (out of 32 RSNs), including 2 posterior components and 1 anterior component, were identified (Supplementary Fig. 1).

Longitudinal Age-related Alterations in FC of MTL Components

We found a dissociation between aMTL and pMTL. A 2 (aMTL vs. pMTL global FC) by 2 (baseline vs. follow-up) ANOVA revealed a significant interaction effect (F (1197) = 129.67, $P < 0.001$; Fig. 2A). A follow-up paired t-test revealed that FC within aMTL declined longitudinally (baseline: 0.05 ± 0.01; follow-up: 0.04 ± 0.01; t (197) = 7.76, $P < 0.001$ [unit of global FC is percent signal changes], whereas FC within pMTL increased (baseline: 0.04 ± 0.008; follow-up: 0.05 ± 0.009; t (197) = 7.41, $P < 0.001$). Similarly, voxel-wise analyses of FC within aMTL and pMTL, respectively, revealed longitudinal decreases (LHC: *XYZ*: −24 −16 −20, t = 8.75; RHC: *XYZ*: 24 −10 −14, t = 3.80, P's<0.05 FDR-corrected over all component-specific voxels) and increases (LPHC: *XYZ*:−12 −22 −18, t =16.67; RPHC: *XYZ*: 22 −30 −18, t = 18.01; P's < 0.05 FDR-corrected over all component-specific voxels; Fig. 2C). Thus, aMTL and pMTL exhibited opposite trajectories of longitudinal changes in FC, with 2 clusters in the aMTL showing decreased FC with the mean aMTL network TC, whereas 2 clusters in the pMTL showed increased FC with the mean pMTL network TC (this effect was observed regardless of whether motion was regressed out pre- or post-ICA (Supplementary Fig. 2).

To further examine longitudinal elevation in pMTL, we extracted an additional ICA-driven measure, which reflects the level of activation (i.e., amplitude) within a network. We found a significant increase in amplitude (baseline: 8.31±4.90; follow-up: 11.36 ± 5.85; t (193) = 7.20, $P < 0.001$). Interestingly, the degree of amplitude increase accelerated with advancing age (Fig. 2B; P-value = 9.7e-09). To investigate the onset of change, we explored the first derivative of the amplitude as a function of age. Using a finite difference approximation along with confidence regions given by ±2 × standard errors of the derivative approximation, we found that the derivative appears to increase from zero Beginning at age 50, but the entire confidence region is above zero at age 60

Internetwork Coupling Between MTL and Cortical DMN

The internetwork connectivity analyses showed a longitudinal decline in internetwork connectivity of the pMTL with anterior (baseline: 0.11 ± 0.21; follow-up: 0.02 ± 0.23; t (193) = 4.71, $P < 0.001$) and posterior (baseline: 0.16±0.18; follow-up: 0.13 ± 0.20; t (193) = 2.05, P = 0.04) cortical DMN components. Thus, with increasing age, the pMTL, which exhibited elevated FC over time, tended to show less FC with the cortical DMNs.

MTL Hyper-connectivity in Relation to GM Volume and Perfusion

Increased pMTL connectivity might be explained by longitudinal changes in GM volume. No significant change–change FC–GM association was found in pMTL ($P > 0.1$). Moreover, elevated FC in pMTL remained significant after controlling for changes in local GM volume (Supplementary Fig. 3). Next, relative CBF (residulized with regard to mean brain CBF) was related to both FC and amplitude in the pMTL. We found significant voxel-wise associations for both elevated and follow-up FC with local CBF in right pMTL (*XYZ*: 28 −32 −12; r (elevated FC, CBF) = 0.24, r (follow-up FC, CBF) = 0.23; $P < 0.001$ (cluster significant at $P < 0.05$ FWE with voxel-wise threshold of $P < 0.001$ (uncorrected)); Fig. 3A). This associations in right pMTL remained significant after controlling for

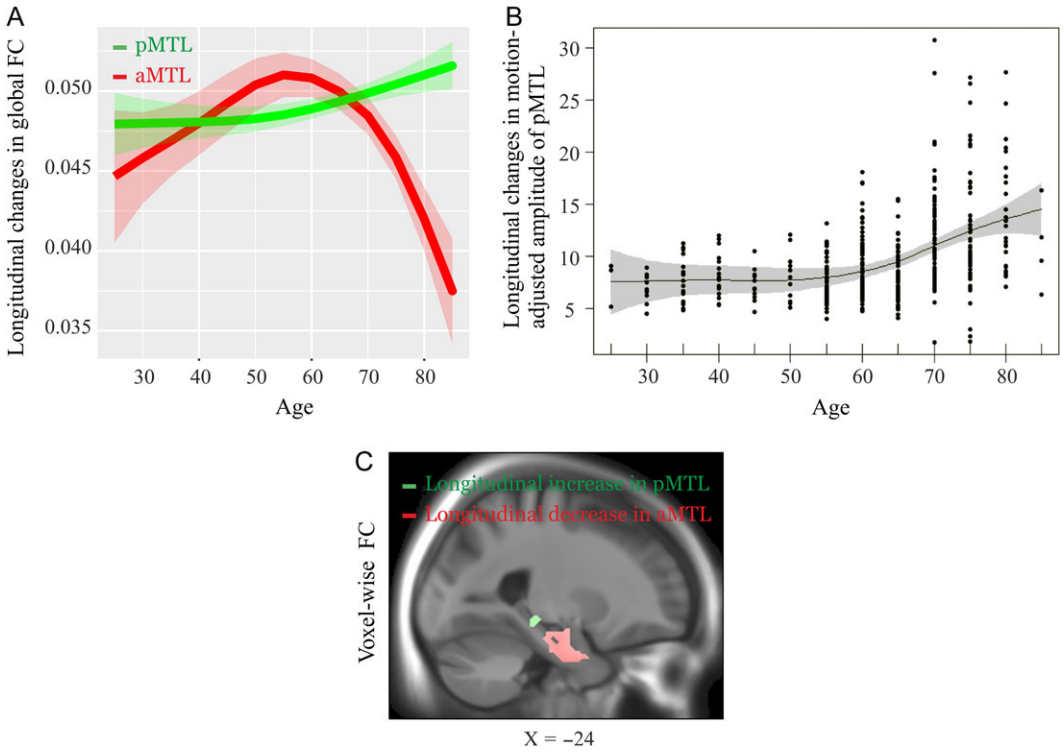

Figure 2. Longitudinal changes of the aMTL and pMTL for 3 different ICA-driven measures (voxel-wise connectivity, global connectivity, and amplitude) after post-ICA motion correction. (*A*) Longitudinal changes in global FC (across the whole RSN shown in Fig. 1) of the aMTL (red) and the pMTL (green). An assumption-free general additive model (GAM) as a function of age was fitted to accurately describe changes across the adult lifespan. The shading represents ± 1 standard error. (*B*) Longitudinal increase in amplitude of the pMTL shown using GAM with a contour reflecting % 95 confidence band. (*C*) voxel-wise changes in FC of the aMTL and pMTL. The slice panel indicates brain regions exhibiting longitudinal decline (in red) and elevation (in green) for the aMTL and the pMTL, respectively. The unit for the global FC is percent signal changes (intensity normalization followed by no scaling; See method section).

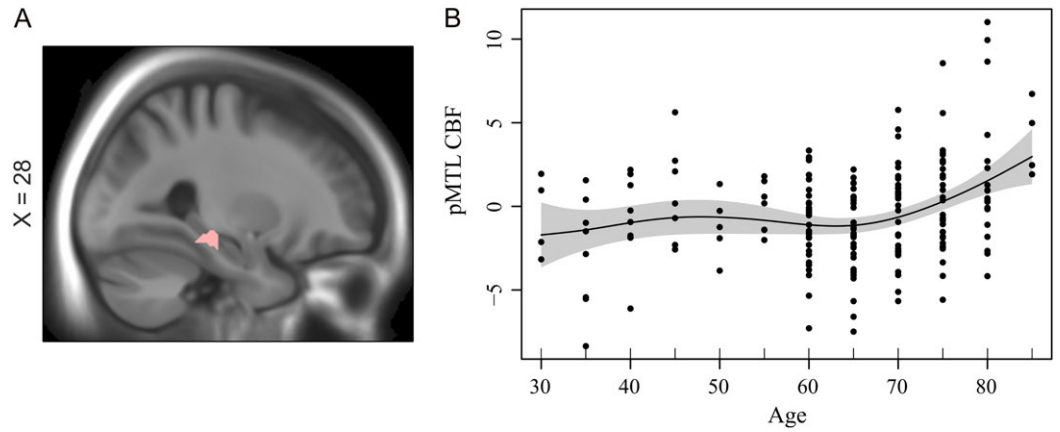

Figure 3. (*A*) Association between FC and CBF in pMTL (*XYZ*: 28 –32 –12; $r = 0.23$, $P = 0.006$). (*B*) Age-related increases in CBF of the pMTL ($P = 7.6\times10^{-5}$). A finite difference approximation of the first derivative along with 95% confidence limits confirmed a reliable increase in pMTL perfusion beginning at age 70 years.

changes in GM volume ($r = 0.23$). Similarly, we also found a significant associations between amplitude and CBF in pMTL ($r = 0.17$, $P = 0.01$). Critically, this association remained significant after controlling for changes in GM volume ($r = 0.15$, $P = 0.02$). As a further assessment of GM volume influences, we eroded the pMTL component SM from which the CBF data was extracted. To do so, we increased the threshold on the pMTL component such that only 15% of top voxels of the original pMTL was preserved. Then, we extracted the average CBF values from this stricter mask. This marginally increased the association between CBF and amplitude ($r = 0.19$, $P = 0.008$), which suggest that the reported result was unlikely to be driven by partial volume effects. An assumption-free GAM model fit indicated age-related increases in perfusion of the pMTL ($P = 7.6\times10^{-5}$; Fig. 3B). A finite difference approximation of the first derivative along with 95%

confidence limits confirmed a reliable increase in pMTL perfusion beginning at age 70 years (this effect was observed after controlling for GM volume; Supplementary Fig. 3D). This finding indicates that elevated FC in the pMTL is metabolically demanding. No age differences in CBF were found for the aMTL (GAM $P = 0.102$; Supplementary Fig.4A)

MTL FC Changes in Relation to Change in Episodic Memory

We examined how episodic-memory change over 15 years related to 5-year changes in FC of the aMTL and pMTL. A voxel-wise analysis of the relation between changes in FC of the pMTL and changes in episodic memory revealed a significant negative association in left parahippacampus (*XYZ*: −28, −26, −18, t=3.20, $P < 0.001$; see Fig. 4), suggesting that individuals with a greater increase in FC showed steeper decline in episodic memory. No significant change–change association was found for the aMTL.

Discussion

The main aim of this study was to investigate whether 5-year longitudinal FC changes would differentially impact the aMTL and pMTL, and in particular whether longitudinal evidence would be obtained for elevated FC in the pMTL. We identified distinct aMTL and pMTL components. Several previous human and animal studies showed structural and functional variations along the anterior–posterior axis of the HC (Moser and Moser 1998; Poppenk and Moscovitch 2011; Blessing et al. 2015; Moscovitch et al. 2016). In addition, neuroimaging studies of the resting brain using high resolution fMRI found fine-grained parcellation of MTL networks in young (Kahn et al. 2008; Libby et al. 2012) and older (Das et al. 2015) adults. Our observation further demonstrates, in an age-heterogeneous sample covering the adult entire lifespan, that MTL contains functionally distinct circuits along the longitudinal axis.

The longitudinal analysis of changes within MTL components revealed an intriguing opposite pattern, such that the degree of FC within the aMTL declined after age 60, whereas elevated FC (and amplitude) was observed within the pMTL. The finding that both networks are vulnerable to aging is in contrast with some previous cross-sectional studies suggesting that age-related alterations only occur in the pMTL (Yassa et al. 2011; Damoiseaux et al. 2016). However, recent RS studies demonstrate that both these MTL networks are affected in the prodromal stage of AD (Das et al. 2015; for review see; Ranganath and Ritchey 2012), with some evidence for elevated FC within MTL subregions in both healthy older adults (Eavani et al. 2016) and MCI patients (Das et al. 2015). MTL has repeatedly been shown to be a part of the widely studied DMN (Greicius et al. 2003; Buckner et al. 2008; Salami et al. 2014). Previous cross-sectional studies indicated heterogeneous effects of age across cortical and MTL DMN subsystems (Campbell et al. 2013; Ferreira and Busatto 2013; Salami et al. 2014). Correspondingly, we found longitudinal support for FC decline of different parts of the cortical DMN (supplementary Fig. 1). Taken together, the current finding provides novel longitudinal evidence that the influence of advancing age is not homogenous within the DMN, or even within MTL DMN subsystems.

The second aim of the study was to investigate the link between FC and perfusion in distinct MTL regions. We hypothesized that elevated MTL FC would be accompanied by a disruption in cortico-MTL FC as well as local MTL hyperperfusion. The analyses of internetwork connectivity between the pMTL with the cortical DMN showed that the degree of coupling between the pMTL with both the anterior and the posterior DMN declined longitudinally. This finding suggests that longitudinal elevation in FC of the pMTL could be a result of reduced cortical input (cf., Salami et al., 2014). It has been argued that elevated HC connectivity might be distally driven by destabilized neural activity in cortical DMN, which might be potentially induced by amyloid accumulation (Palop and Mucke 2010). Thus, it seems plausible that elevated FC in pMTL resulted from less cortical inhibitory signal. Moreover, previous studies have reported coupling of FC and regional CBF, which provide a direct and quantitative measures of physiology and metabolism of RSNs (Liang et al. 2013; Jann et al. 2015). Our analyses of the relation between both changes and follow-up FC with perfusion revealed a positive association in pMTL, suggesting a tight coupling between blood supply and FC. The latter along with the finding of age-related increased perfusion of the posterior MTL suggest that increased FC in pMTL is a metabolically demanding alteration. A recent study found that cortical disinhibition was associated with increased metabolic demands

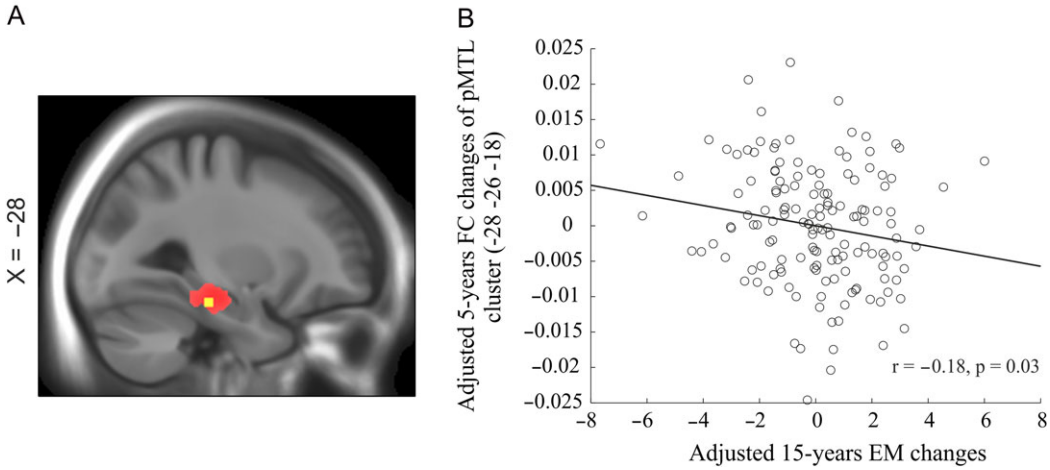

Figure 4. Changes in episodic memory in relation to changes in FC of the pMTL. (A) The slide panel indicates a brain regions (in yellow) of the whole pMTL (in red) in which longitudinal changes in FC are associated with changes in episodic memory. (B) Scatter plot displays change–change association between FC of the pMTL and episodic memory.

in the HC (Gilani et al. 2014). Thus our finding of age-related hyperperfusion further supports that reduced cortical inhibition of the pMTL underlies age-related increases in FC. Additionally, elevated MTL resting perfusion has been reported for non-demented elderly individuals with increased risk for AD (Fleisher et al. 2009), patients with MCI (Lacalle-Aurioles et al. 2014), and AD (Alsop et al. 2008). Our cross-sectional finding suggests that elevated perfusion in MTL might be a continuum between normal cognitive aging, MCI, and AD. In spite of an important overlap in pMTL across normal and pathological aging, noteworthy discrepancies found for perfusion profiles of other critical large-scale networks such as the posterior DMN. Whereas hypometabolism in the PCC have been consistently reported in MCI and AD (Jagust and Landau 2012; Lacalle-Aurioles et al. 2014), preserved PCC metabolism was found in the current study (Supplementary Fig. 4B), which confirms differences in perfusion profile of AD patients and healthy individuals in our sample.

A final purpose of the study was to longitudinally examine the link between individual differences in 5-year change in MTL FC and 15-year change in hippocampus-based episodic long-term memory. The results revealed a negative association between changes in pMTL and EM. This finding contrasts with a positive association found between homotopic hippocampal connectivity and free recall in a sample of young individuals (Wang et al. 2010), but concurs with our previous cross-sectional result that elevated MTL connectivity is detrimental for episodic memory in elderly people (Salami et al. 2014). Also, a recent longitudinal RS study showed that memory changes were related to altered FC in an age-dependent manner, although the underlying mechanism remained to be specified (Fjell et al. 2015). A plausible mechanism underlying negative association between changes in EM and changes in FC, as shown in our previous study, is that elevated MTL connectivity in aging at rest leads to failure in hippocampal decoupling (i.e., prevention in efficient hippocampal-cortical connectivity) during active task, which in turn cascades into age-related decline in EM performance (Westlye et al. 2011; Salami et al. 2014). More specifically, elevated hippocampal coupling at rest was associated with reduced functional integration of HC with other regions, such as the prefrontal cortex, during EM encoding (Salami et al. 2014). Speculatively, elevated FC in PMTLmight be due to progressively less inhibitory cortical input. Reduced inhibitory input has been shown to lead to increased FC in motor cortex in studies of amyotrophic lateral sclerosis (ALS; (Douaud et al. 2011)). Critically, in the context of aging, it has also been proposed that MTL subregions are vulnerable to age-related loss of inhibitory input, which cascades into MTL hyperactivation (Leal and Yassa 2013). Despite negative EM-FC change–change association in the pMTL, no association was found for the aMTL. Relatedly, it has been proposed that pMTL is more likely to be involved in memory, whereas the anterior hippocampus is more involved in other complex behaviors such as emotion, sensory-motor integration and goal-directed activity (Bast and Feldon 2003; Fanselow and Dong 2010; Lau et al. 2010; Small et al. 2011). Another line of research, however, suggested that aMTL is more engaged during associative memory encoding (Chua et al. 2007; Salami et al. 2012), whereas pMTL is more activated during item memory retrieval (Sheldon and Levine 2015). The dichotomy view of functional role of the MTL longitudinal axis has recently been seriously challenged (Strange et al. 2014), and thus call for new research to determine the precise contribution of distinct parts of MTL to long-term memory system.

In summary, our results provide the first longitudinal evidence for opposing effects of advancing age on FC of the pMTL and aMTL. The elevated FC in pMTL, which was accompanied by local increase in perfusion was detrimental for episodic memory performance, and could thus be served as a sign of brain dysfunction in aging that precedes emergence of clinical manifestation.

Supplementary Material

Supplementary material can be found at: http://www.cercor.oxfordjournals.org/

Funding

Swedish Research Council, Knut and Alice Wallenberg Foundation Torsten, Ragnar Söderberg's foundation, and Västerbotten County Council.

Notes

We thank the staff of the BETULA project, and the staff at the Umeå Center for Functional Brain Imaging. *Conflict of Interest*: None declared.

References

Achard S, Bullmore E. 2007. Efficiency and cost of economical brain functional networks. PLoS Comput Biol. 3:e17.

Allen EA, Damaraju E, Plis SM, Erhardt EB, Eichele T, Calhoun VD. 2014. Tracking whole-brain connectivity dynamics in the resting state. Cereb Cortex. 24:663–676.

Allen EA, Erhardt EB, Damaraju E, Gruner W, Segall JM, Silva RF, Havlicek M, Rachakonda S, Fries J, Kalyanam R, et al. 2011. A baseline for the multivariate comparison of resting-state networks. Front Syst Neurosci. 5:2.

Allen EA, Erhardt EB, Wei Y, Eichele T, Calhoun VD. 2012. Capturing inter-subject variability with group independent component analysis of fMRI data: a simulation study. Neuroimage. 59:4141–4159.

Alsop DC, Casement M, de Bazelaire C, Fong T, Press DZ. 2008. Hippocampal hyperperfusion in Alzheimer's disease. Neuroimage. 42:1267–1274.

Andrews-Hanna JR, Reidler JS, Sepulcre J, Poulin R, Buckner RL. 2010. Functional-anatomic fractionation of the brain's default network. Neuron. 65:550–562.

Andrews-Hanna JR, Snyder AZ, Vincent JL, Lustig C, Head D, Raichle ME, Buckner RL. 2007. Disruption of large-scale brain systems in advanced aging. Neuron. 56:924–935.

Ashburner J. 2007. A fast diffeomorphic image registration algorithm. Neuroimage. 38:95–113.

Balsters JH, O'Connell RG, Galli A, Nolan H, Greco E, Kilcullen SM, Bokde AL, Lai R, Upton N, Robertson IH. 2013. Changes in resting connectivity with age: a simultaneous electroencephalogram and functional magnetic resonance imaging investigation. Neurobiol Aging. 34:2194–2207.

Bast T, Feldon J. 2003. Hippocampal modulation of sensorimotor processes. Prog Neurobiol. 70:319–345.

Basu J, Zaremba JD, Cheung SK, Hitti FL, Zemelman BV, Losonczy A, Siegelbaum SA. 2016. Gating of hippocampal activity, plasticity, and memory by entorhinal cortex long-range inhibition. Science. 351:aaa5694.

Bäckman L, Lindenberger U, Li SC, Nyberg L. 2010. Linking cognitive aging to alterations in dopamine neurotransmitter

functioning: recent data and future avenues. Neurosci Biobehav Rev. 34:670–677.
Bäckman L, Nyberg L, Lindenberger U, Li SC, Farde L. 2006. The correlative triad among aging, dopamine, and cognition: current status and future prospects. Neurosci Biobehav Rev. 30:791–807.
Bell AJ, Sejnowski TJ. 1995. An information-maximization approach to blind separation and blind deconvolution. Neural Comput. 7:1129–1159.
Biswal BB, Mennes M, Zuo XN, Gohel S, Kelly C, Smith SM, Beckmann CF, Adelstein JS, Buckner RL, Colcombe S, et al. 2010. Toward discovery science of human brain function. Proc Natl Acad Sci USA. 107:4734–4739.
Blessing EM, Beissner F, Schumann A, Brunner F, Bar KJ. 2015. A data-driven approach to mapping cortical and subcortical intrinsic functional connectivity along the longitudinal hippocampal axis. Hum Brain Mapp. 37:462–476.
Boraxbekk CJ, Salami A, Wahlin A, Nyberg L. 2015. Physical activity over a decade modifies age-related decline in perfusion, gray matter volume, and functional connectivity of the posterior default-mode network-A multimodal approach. NeuroImage. 131:133–141.
Buckner RL, Andrews-Hanna JR, Schacter DL. 2008. The brain's default network: anatomy, function, and relevance to disease. Ann NY Acad Sci. 1124:1–38.
Buckner RL, Krienen FM, Yeo BT. 2013. Opportunities and limitations of intrinsic functional connectivity MRI. Nat Neurosci. 16:832–837.
Calhoun VD, Adali T, Pearlson GD, Pekar JJ. 2001a. A method for making group inferences from functional MRI data using independent component analysis. Hum Brain Mapp. 14:140–151.
Calhoun VD, Adali T, Pearlson GD, Pekar JJ. 2001b. Spatial and temporal independent component analysis of Functional MRI data containing a pair of task-related waveforms. Hum Brain Mapp. 13:43–53.
Campbell KL, Grigg O, Saverino C, Churchill N, Grady CL. 2013. Age differences in the intrinsic functional connectivity of default network subsystems. Front Aging Neurosci. 5:73.
Casanova R, Srikanth R, Baer A, Laurienti PJ, Burdette JH, Hayasaka S, Flowers L, Wood F, Maldjian JA. 2007. Biological parametric mapping: a statistical toolbox for multimodality brain image analysis. Neuroimage. 34:137–143.
Chua EF, Schacter DL, Rand-Giovannetti E, Sperling RA. 2007. Evidence for a specific role of the anterior hippocampal region in successful associative encoding. Hippocampus. 17:1071–1080.
Damoiseaux JS, Beckmann CF, Arigita EJ, Barkhof F, Scheltens P, Stam CJ, Smith SM, Rombouts SA. 2008. Reduced resting-state brain activity in the "default network" in normal aging. Cereb Cortex. 18:1856–1864.
Damoiseaux JS, Viviano RP, Yuan P, Raz N. 2016. Differential effect of age on posterior and anterior hippocampal functional connectivity. Neuroimage. 133:468–476.
Das SR, Pluta J, Mancuso L, Kliot D, Orozco S, Dickerson BC, Yushkevich PA, Wolk DA. 2013. Increased functional connectivity within medial temporal lobe in mild cognitive impairment. Hippocampus. 23:1–6.
Das SR, Pluta J, Mancuso L, Kliot D, Yushkevich PA, Wolk DA. 2015. Anterior and posterior MTL networks in aging and MCI. Neurobiol Aging. 36:S141–S150.e141.
Di X, Biswal BB. 2014. Modulatory interactions between the default mode network and task positive networks in resting-state. PeerJ. 2:e367.
Douaud G, Filippini N, Knight S, Talbot K, Turner MR. 2011. Integration of structural and functional magnetic resonance imaging in amyotrophic lateral sclerosis. Brain. 134:3470–3479.
Eavani H, Hsieh MK, An Y, Erus G, Beason-Held L, Resnick S, Davatzikos C. 2016. Capturing heterogeneous group differences using mixture-of-experts: application to a study of aging. Neuroimage. 125:498–514.
Erhardt EB, Rachakonda S, Bedrick EJ, Allen EA, Adali T, Calhoun VD. 2011. Comparison of multi-subject ICA methods for analysis of fMRI data. Hum Brain Mapp. 32:2075–2095.
Fanselow MS, Dong HW. 2010. Are the dorsal and ventral hippocampus functionally distinct structures? Neuron. 65:7–19.
Ferreira LK, Busatto GF. 2013. Resting-state functional connectivity in normal brain aging. Neurosci Biobehav Rev. 37:384–400.
Ferreira LK, Regina AC, Kovacevic N, Martin MD, Santos PP, Carneiro CG, Kerr DS, Amaro E Jr, McIntosh AR, Busatto GF. 2015. Aging effects on whole-brain functional connectivity in adults free of cognitive and psychiatric disorders. Cerebral cortex. bhv190.
Fjell AM, Sneve MH, Grydeland H, Storsve AB, de Lange AG, Amlien IK, Rogeberg OJ, Walhovd KB. 2015. Functional connectivity change across multiple cortical networks relates to episodic memory changes in aging. Neurobiol Aging. 36:3255–3268.
Fjell AM, Walhovd KB, Fennema-Notestine C, McEvoy LK, Hagler DJ, Holland D, Brewer JB, Dale AM. 2009. One-year brain atrophy evident in healthy aging. J Neurosci. 29:15223–15231.
Fleisher AS, Podraza KM, Bangen KJ, Taylor C, Sherzai A, Sidhar K, Liu TT, Dale AM, Buxton RB. 2009. Cerebral perfusion and oxygenation differences in Alzheimer's disease risk. Neurobiol Aging. 30:1737–1748.
Geerligs L, Renken RJ, Saliasi E, Maurits NM, Lorist MM. 2014. A brain-wide study of age-related changes in functional connectivity. Cereb Cortex. 25:1987–1999.
Geerligs L, Saliasi E, Renken RJ, Maurits NM, Lorist MM. 2014. Flexible connectivity in the aging brain revealed by task modulations. Hum Brain Mapp. 35:3788–3804.
Gilani A, Chohan MO, Inan M, Schobel SA, Chaudhury NH, Paskewitz S, Chuhma N, Glickstein S, Merker RJ, Xu Q, et al. 2014. Interneuron precursor transplants in adult hippocampus reverse psychosis-relevant features in a mouse model of hippocampal disinhibition. Proc Nat Acad Sci. 111:7450–7455.
Glahn DC, Winkler AM, Kochunov P, Almasy L, Duggirala R, Carless MA, Curran JC, Olvera RL, Laird AR, Smith SM, et al. 2010. Genetic control over the resting brain. Proc Natl Acad Sci USA. 107:1223–1228.
Grady C. 2012. The cognitive neuroscience of ageing. Nat Rev Neurosci. 13:491–505.
Greicius MD, Krasnow B, Reiss AL, Menon V. 2003. Functional connectivity in the resting brain: a network analysis of the default mode hypothesis. Proc Natl Acad Sci USA. 100:253–258.
Himberg J, Hyvarinen A, Esposito F. 2004. Validating the independent components of neuroimaging time series via clustering and visualization. Neuroimage. 22:1214–1222.
Jafri MJ, Pearlson GD, Stevens M, Calhoun VD. 2008. A method for functional network connectivity among spatially independent resting-state components in schizophrenia. Neuroimage. 39:1666–1681.

Jagust WJ, Landau SM. 2012. Apolipoprotein E, not fibrillar beta-amyloid, reduces cerebral glucose metabolism in normal aging. J Neurosci. 32:18227–18233.

Jann K, Gee DG, Kilroy E, Schwab S, Smith RX, Cannon TD, Wang DJ. 2015. Functional connectivity in BOLD and CBF data: similarity and reliability of resting brain networks. Neuroimage. 106:111–122.

Josefsson M, de Luna X, Pudas S, Nilsson LG, Nyberg L. 2012. Genetic and lifestyle predictors of 15-year longitudinal change in episodic memory. J Am Geriatr Soc. 60:2308–2312.

Kahn I, Andrews-Hanna JR, Vincent JL, Snyder AZ, Buckner RL. 2008. Distinct cortical anatomy linked to subregions of the medial temporal lobe revealed by intrinsic functional connectivity. J Neurophysiol. 100:129–139.

Kalpouzos G, Chetelat G, Baron JC, Landeau B, Mevel K, Godeau C, Barre L, Constans JM, Viader F, Eustache F, et al. 2009. Voxel-based mapping of brain gray matter volume and glucose metabolism profiles in normal aging. Neurobiol Aging. 30:112–124.

Koch W, Teipel S, Mueller S, Buerger K, Bokde AL, Hampel H, Coates U, Reiser M, Meindl T. 2010. Effects of aging on default mode network activity in resting state fMRI: does the method of analysis matter? Neuroimage. 51:280–287.

Lacalle-Aurioles M, Mateos-Perez JM, Guzman-De-Villoria JA, Olazaran J, Cruz-Orduna I, Aleman-Gomez Y, Martino ME, Desco M. 2014. Cerebral blood flow is an earlier indicator of perfusion abnormalities than cerebral blood volume in Alzheimer's disease. J Cereb Blood Flow Metab. 34:654–659.

Lau JY, Goldman D, Buzas B, Hodgkinson C, Leibenluft E, Nelson E, Sankin L, Pine DS, Ernst M. 2010. BDNF gene polymorphism (Val66Met) predicts amygdala and anterior hippocampus responses to emotional faces in anxious and depressed adolescents. Neuroimage. 53:952–961.

Leal SL, Yassa MA. 2013. Perturbations of neural circuitry in aging, mild cognitive impairment, and Alzheimer's disease. Ageing Res Rev. 12:823–831.

Liang X, Zou Q, He Y, Yang Y. 2013. Coupling of functional connectivity and regional cerebral blood flow reveals a physiological basis for network hubs of the human brain. Proc Natl Acad Sci USA. 110:1929–1934.

Libby LA, Ekstrom AD, Ragland JD, Ranganath C. 2012. Differential connectivity of perirhinal and parahippocampal cortices within human hippocampal subregions revealed by high-resolution functional imaging. J Neurosci. 32:6550–6560.

Lindenberger U, von Oertzen T, Ghisletta P, Hertzog C. 2011. Cross-sectional age variance extraction: what's change got to do with it? Psychol Aging. 26:34–47.

Mayer AR, Ling JM, Allen EA, Klimaj SD, Yeo RA, Hanlon FM. 2015. Static and dynamic intrinsic connectivity following mild traumatic brain injury. J Neurotrauma. 32:1046–1055.

Moscovitch M, Cabeza R, Winocur G, Nadel L. 2016. Episodic memory and Beyond: the hippocampus and neocortex in transformation. Annu Rev Psychol. 67:105–134.

Moser MB, Moser E. 1998. Functional differentiation in the hippocampus. Hippocampus. 8:608–619.

Mousavi M, Jonsson P, Antti H, Adolfsson R, Nordin A, Bergdahl J, Eriksson K, Moritz T, Nilsson LG, Nyberg L. 2014. Serum metabolomic biomarkers of dementia. Dement Geriatr Cogn Dis Extra. 4:252–262.

Mowinckel AM, Espeseth T, Westlye LT. 2012. Network-specific effects of age and in-scanner subject motion: a resting-state fMRI study of 238 healthy adults. NeuroImage. 63:1364–1373.

Nilsson L-G, Adolfsson R, Backman L, de Frias C, Molander B, Nyberg L. 2004. Betula: a prospective cohort study on memory, health and aging. Aging Neuropsychol Cogn. 11:134–148.

Nilsson L-G, Bäckman L, Erngrund K, Nyberg L, Adolfsson R, Bucht G, Karlsson S, Widing M, Winblad B. 1997. The betula prospective cohort study: memory, health, and aging. Aging Neuropsychol Cogn. 4:1–32.

Nyberg L, Andersson M, Kauppi K, Lundquist A, Persson J, Pudas S, Nilsson LG. 2014. Age-related and genetic modulation of frontal cortex efficiency. J Cogn Neurosci. 26: 746–754.

Nyberg L, Maitland SB, Rönnlund M, Bäckman L, Dixon RA, Wahlin Å, Nilsson L-G. 2003. Selective adult age differences in an age-invariant multifactor model of declarative memory. Psychol Aging. 18:149–160.

Nyberg L, Salami A, Andersson M, Eriksson J, Kalpouzos G, Kauppi K, Lind J, Pudas S, Persson J, Nilsson L-G. 2010. Longitudinal evidence for diminished frontal cortex function in aging. Proc Nat Acad Sci. 107:22682–22686.

Palop JJ, Mucke L. 2010. Amyloid-beta-induced neuronal dysfunction in Alzheimer's disease: from synapses toward neural networks. Nat Neurosci. 13:812–818.

Passow S, Specht K, Adamsen TC, Biermann M, Brekke N, Craven AR, Ersland L, Gruner R, Kleven-Madsen N, Kvernenes OH, et al. 2015. Default-mode network functional connectivity is closely related to metabolic activity. Hum Brain Mapp. 36:2027–2038.

Poppenk J, Evensmoen HR, Moscovitch M, Nadel L. 2013. Long-axis specialization of the human hippocampus. Trends Cogn Sci. 17:230–240.

Poppenk J, Moscovitch M. 2011. A hippocampal marker of recollection memory ability among healthy young adults: contributions of posterior and anterior segments. Neuron. 72:931–937.

Power JD, Barnes KA, Snyder AZ, Schlaggar BL, Petersen SE. 2012. Spurious but systematic correlations in functional connectivity MRI networks arise from subject motion. Neuroimage. 59:2142–2154.

Pudas S, Persson J, Nilsson LG, Nyberg L. 2014. Midlife memory ability accounts for brain activity differences in healthy aging. Neurobiol Aging. 35:2495–2503.

Ranganath C, Ritchey M. 2012. Two cortical systems for memory-guided behaviour. Nat Rev Neurosci. 13:713–726.

Raz N, Lindenberger U, Rodrigue KM, Kennedy KM, Head D, Williamson A, Dahle C, Gerstorf D, Acker JD. 2005. Regional brain changes in aging healthy adults: general trends, individual differences and modifiers. Cereb Cortex. 15: 1676–1689.

Salami A, Eriksson J, Nilsson LG, Nyberg L. 2011. Age-related white matter microstructural differences partly mediate age-related decline in processing speed but not cognition. Biochim Biophys Acta. 1822:408–415.

Salami A, Eriksson J, Nyberg L. 2012. Opposing effects of aging on large-scale brain systems for memory encoding and cognitive control. J Neurosci. 32:10749–10757.

Salami A, Pudas S, Nyberg L. 2014. Elevated hippocampal resting-state connectivity underlies deficient neurocognitive function in aging. Proc Natl Acad Sci USA. 111: 17654–17659.

Salami A, Rieckmann A, Fischer H, Backman L. 2013. A multivariate analysis of age-related differences in functional networks supporting conflict resolution. NeuroImage. 86:150–163.

Segobin S, La Joie R, Ritz L, Beaunieux H, Desgranges B, Chetelat G, Pitel AL, Eustache F. 2015. FDG-PET contributions to the

pathophysiology of memory impairment. Neuropsychol Rev. 25:326–355.

Sheldon S, Levine B. 2015. The medial temporal lobes distinguish between within-item and item-context relations during autobiographical memory retrieval. Hippocampus. 25:1577–1590.

Small SA, Schobel SA, Buxton RB, Witter MP, Barnes CA. 2011. A pathophysiological framework of hippocampal dysfunction in ageing and disease. Nat Rev Neurosci. 12:585–601.

Strange BA, Witter MP, Lein ES, Moser EI. 2014. Functional organization of the hippocampal longitudinal axis. Nat Rev Neurosci. 15:655–669.

Toussaint PJ, Maiz S, Coynel D, Doyon J, Messe A, de Souza LC, Sarazin M, Perlbarg V, Habert MO, Benali H. 2014. Characteristics of the default mode functional connectivity in normal ageing and Alzheimer's disease using resting state fMRI with a combined approach of entropy-based and graph theoretical measurements. Neuroimage. 101:778–786.

Van Dijk KR, Sabuncu MR, Buckner RL. 2012. The influence of head motion on intrinsic functional connectivity MRI. Neuroimage. 59:431–438.

Wang L, Negreira A, LaViolette P, Bakkour A, Sperling RA, Dickerson BC. 2010. Intrinsic interhemispheric hippocampal functional connectivity predicts individual differences in memory performance ability. Hippocampus. 20:345–351.

Westlye ET, Lundervold A, Rootwelt H, Lundervold AJ, Westlye LT. 2011. Increased hippocampal default mode synchronization during rest in middle-aged and elderly APOE epsilon4 carriers: relationships with memory performance. J Neurosci. 31:7775–7783.

Yan CG, Cheung B, Kelly C, Colcombe S, Craddock RC, Di Martino A, Li Q, Zuo XN, Castellanos FX, Milham MP. 2013. A comprehensive assessment of regional variation in the impact of head micromovements on functional connectomics. Neuroimage. 76:183–201.

Yassa MA, Mattfeld AT, Stark SM, Stark CE. 2011. Age-related memory deficits linked to circuit-specific disruptions in the hippocampus. Proc Natl Acad Sci USA. 108:8873–8878.

Zarrinkoob L, Ambarki K, Wahlin A, Birgander R, Eklund A, Malm J. 2015. Blood flow distribution in cerebral arteries. J Cereb Blood Flow Metab. 35:648–654.